UNIVERSITY OF LEEDS

This is a repository copy of *Stage-Discharge Prediction for Converging Compound Channels with Narrow Floodplains*.

White Rose Research Online URL for this paper:
http://eprints.whiterose.ac.uk/126630/

Version: Accepted Version

Article:
Naik, B, Khatua, KK, Wright, NG et al. (1 more author) (2017) Stage-Discharge Prediction for Converging Compound Channels with Narrow Floodplains. Journal of Irrigation and Drainage Engineering, 143 (8). 04017017. ISSN 0733-9437

https://doi.org/10.1061/(ASCE)IR.1943-4774.0001184

(c) 2017, American Society of Civil Engineers. This is an author produced version of a paper published in the Journal of Irrigation and Drainage Engineering. Uploaded in accordance with the publisher's self-archiving policy. This material may be downloaded for personal use only. Any other use requires prior permission of the American Society of Civil Engineers. This material may be found at: https://doi.org/10.1061/(ASCE)IR.1943-4774.0001184

Reuse
Unless indicated otherwise, fulltext items are protected by copyright with all rights reserved. The copyright exception in section 29 of the Copyright, Designs and Patents Act 1988 allows the making of a single copy solely for the purpose of non-commercial research or private study within the limits of fair dealing. The publisher or other rights-holder may allow further reproduction and re-use of this version - refer to the White Rose Research Online record for this item. Where records identify the publisher as the copyright holder, users can verify any specific terms of use on the publisher's website.

Takedown
If you consider content in White Rose Research Online to be in breach of UK law, please notify us by emailing eprints@whiterose.ac.uk including the URL of the record and the reason for the withdrawal request.

White Rose university consortium
Universities of Leeds, Sheffield & York

eprints@whiterose.ac.uk
https://eprints.whiterose.ac.uk/

IR7753

Stage-Discharge Prediction for Converging Compound Channels with Narrow Floodplains

B. Naik[1], K. K. Khatua[2], N. G. Wright[3], and A. Sleigh[4]

1 Ph.D. Research Scholar, Department of Civil Engineering, National Institute of Technology Rourkela, India (corresponding author). Email: banditanaik1982@gmail.com

2 Associate Professor, Department of Civil Engineering, National Institute of Technology Rourkela, India. Email: kkkhatua@yahoo.com

3 Professor of Water and Environmental Engineering, University of Leeds, School of Civil Engineering, UK. Email: n.g.wright@leeds.ac.uk

4 Professor, Department of Water and Environmental Engineering, University of Leeds, School of Civil Engineering, UK. Email: p.a.sleigh@leeds.ac.uk

ABSTRACT: Momentum transfer between the main channel and the side flood plains tends to increase the floodplain shear whereas the main channel shear decreases. The increase and decrease in shear are greatly influenced when a compound channel is with non-prismatic flood plains. In converging compound channels water flow on the floodplain crosses over water flow in the main channel, resulting in increased interactions and momentum exchanges. An experimental analysis concerning the distribution of shear stress in the main channel and floodplain for both prismatic and non-prismatic compound channels under different over-bank flow conditions are performed. New equations are developed for predicting boundary shear

stress distribution for a compound channel with the non-prismatic flood plain. Using these expressions the stage-discharge relationships for both prismatic and non-prismatic compound channels of lower width ratio have been successfully estimated. The efficiency of the models has also been verified by applying natural river data sets.

Author Keywords: overbank flow, boundary shear, stage discharge, Prismatic, non-prismatic, low width ratio

INTRODUCTION

Compound channels are the usual pattern of rivers during floods. These are very vital for environmental, ecological and design issue. It has become essential to study the flow behavior of rivers both in inbank and overbank flow conditions. Sellin (1964) first demonstrated the momentum transfer phenomena in a compound channel on the basis of experimental investigation. After that many investigators proved that momentum transfer mechanism causes the non-uniformity of the boundary shear stress distribution along the subsection perimeters. Knight and Hamed (1984) proposed boundary shear distribution models for both homogeneous and non-homogeneous compound channels of width ratio α (α =width ratio = Flood plain width (B)/ main channel width (b)) value up to 4. Mohanty et al. (2014) found a new expression of boundary shear distribution for compound channel of width ratio α up to 11.96. When these expressions are used for lower width ratio prismatic and non-prismatic compound channels, significant errors were observed in estimation of shear distribution due to not accounting the mass and momentum transfer (Bousmar and Zech (1999), Bousmar et al. (2004), Rezaei (2006)

and Proust et al. (2006)). These important factors should be considered in the flow modeling for the non-prismatic compound channel. Experiments have been conducted on compound channels with various converging flood plains to obtain expressions for $\%S_{fp}$ ($\%S_{fp} = 100\times S_{fp} / SF$, S_{fp} = boundary shear force occurring in the floodplains and SF the total shear force of the compound cross section) and finally, procedure has been given for stage discharge prediction for the compound channel of low width ratio for both prismatic and non-prismatic flood plain.

EXPERIMENTAL WORKS

Experimental Procedure

Experiments on non-prismatic compound channel have been performed at the Hydraulics and Fluid mechanics Laboratory of National Institute of Technology, Rourkela, India. Three sets of compound channels with converging floodplains made up of Perspex sheet were fabricated inside a concrete flume of size 15m long × 0.9m width × 0.5m depth. The upstream part of the non-prismatic compound channel was considered for taking a measurement of the prismatic part. The width ratio of the prismatic part of the compound channel was found to be α = 1.8 and the aspect ratio of the main channel were found to be δ = 5 (δ =aspect ratio =main channel width (b) / main channel height (h)) which was maintained constant throughout the length. Keeping the geometry of main channel constant, the converging angles of the flood plains were changed to 12.38°, 9^o and 5^0 respectively. The converging length of the fabricated channels was estimated to be 0.84m, 1.26m and 2.28m respectively. Longitudinal bed slope of the channel was maintained at 0.0011, satisfying subcritical flow conditions. The roughness of the floodplain and main channel were alike and the Manning's n was find out as 0.011 from the inbank experimental runs

in the channel. A complete re-circulating system of water supply from the underground sump to the channels through overhead tank and volumetric tank was done with the series of centrifugal pumps. In the upstream section of the rectangular notch flow strengtheners were provided to reduce the turbulence and velocity approach. At the downstream end of the channel an adjustable tailgate was present to maintain the uniform flow throughout the test reach of the channel. Water flowing over the channel was collected by a volumetric tank that helps to record the discharge by time rise method. Figure 1(a) shows the plan view of the experimental setup. Figure1 (b) shows the Longitudinal & Cross-sectional dimension of the non-prismatic compound channels. Figure 1(c) Grid showing the velocity measurement at the test section. A series of micro-Pitot tubes of 4.77 mm external diameter in combination with suitably inclined manometers as well as 16-MHz Micro-ADV (Acoustic Doppler Velocity-meter) were used to measure velocity at the predefined flow-grid points. Boundary shear stresses were measured at the predefined boundary points along the wetted perimeter of the compound channels using Patel's (1965) relationship. Summary of geometrical parameters of present experimental channels (both prismatic and non-prismatic) with details of other investigators channels are given in Table 1 and Table 2 respectively.

EXPERIMENTAL RESULTS

Stage-discharge relationship for both prismatic and non-prismatic section are shown in Figure 2(a) and 2(b) respectively. A total 15 number of runs are observed at these test reaches. Using the stage-discharge data for the NITR series (both for prismatic and non-prismatic sections), a line of best-fit curves were obtained mathematically in the form of a simple power function. A

typical longitudinal velocity contour of the prismatic section with relative depth 0.15 is shown in Figure 2(c). The maximum point's velocities are found to occur near the middle free surface of the main channel and minimum velocities are found to be at the corners of flood plains. This is because of the converging flood plain from both sides which accelerates the flow diverting to the main channel sections. At the non-prismatic sections i.e.section-2, the boundary shears distribution for a typical case of relative flow depth 0.15 for converging floodplain angle 12. 38º and of relative depth 0.5 for the converging angle 11.31° of Rezaei (2006) are shown in Figure 3(a) and 3(b) respectively. These data are useful for examining the force balance along the channel, for calibration of the numerical model and for finding the location of secondary flow cells. Looking to the boundary shear distribution in Figure 3(a) it can be observed that there is a peak at the mid of the main channel and the value decreases towards the flood plain regions. There is a sudden drop of boundary shear value noticed at the interfaces. This happened to all the experimental section covering from prismatic to non-prismatic parts. Further from sec-1 to sec-3, the peak value of boundary shear stress is found to increases. The nature of boundary shear stress distribution is a little bit different in Figure 3(b). At sec-1of Rezaei (2006) channel, the pattern of boundary shear stress distribution is similar to that of NITR channel results however at the last section the peak value is not at the mid of the main channel but at the interfaces i.e. particularly at the turbulent region. This is due to that Rezaei (2006) channel bears higher aspect ratio where as NITR channel has a lower aspect ratio as well as due to the higher slope of NITR channel as compared to Rezaei (2006) channel. This also occurred due to higher order of secondary flow that occurs at the corner of the main channel and at the interfaces.

BOUNDARY SHEAR DISTRIBUTION

Compound channel with Prismatic Flood Plain

Different boundary sections of the compound channel for both prismatic and non-prismatic sections involving the wetted parameters are labelled as (1), (2), (3) and (4) are presented in Figure (4). Label (1) indicates the two vertical edges of the floodplain [2(H- h)], and (2) indicates floodplain beds (B - b). Label (3) indicates the two main channel height (2h) and the width of the main channel bed (b) is indicated by label (4) (where H = Total height of the compound channel, B = Total width of the compound channel). To find out the relevant boundary shear force per unit length for each element experimental shear stress distributions at each point of the wetted perimeter are numerically integrated over the respective sub-lengths of each boundary element (l), (2), (3) and (4). Total boundary shear forces have been computed by adding all the beds and walls of the compound channel. Then it has been used as a divisor to calculate the percentages of shear force carried by the boundary elements of the compound channel. Percentage of shear force by floodplains comprising elements (1) and (2) is represented as $\%S_{fp}$. An equation of $\%S_{fp}$ with α and β (β = relative depth = (H- h)/H) for lower width prismatic compound channels have now been obtained. Formerly different researchers have presented their model for $\%S_{fp}$. Knight and Demetriou (1983) proposed an equation for $\%S_{fp}$

$$\%S_{fp} = 48(\alpha - 0.8)^{0.289}(2\beta)^{m} \quad (1)$$

Where m is calculated from the relation

$$m = 1/[0.75e^{0.38\,\alpha}] \quad (2)$$

Equation (1) is relevant for homogeneous compound channels. Again Knight and Hamed (1984) developed a new equation for non-homogeneous compound channels

$$\%S_{fp} = 48(\alpha - 0.8)^{0.289}(2\beta)^{m}[1 + 1.02\sqrt{\beta}\log\gamma] \quad (3)$$

Where γ = Ratio of Manning's roughness of floodplain (n_{fp}) and the Manning's roughness of main channel (n_{mc})

Equation (1) is useful for $\alpha \leq 4$. Khatua and Patra (2007) developed equation (3) for α up to = 5.25

$$\%S_{fp} = 1.23(\beta)^{0.1833}(38Ln\alpha + 3.6262)[1 + 1.02\sqrt{\beta}\log\gamma] \quad (4)$$

Khatua et al (2012) developed a new equation for $\%S_{fp}$ for α = 6.67

$$\%S_{fp} = 4.1045(\%A_{fp})^{0.691} \quad (5)$$

Mohanty et al. (2014) again proposed a model for α up to 12

$$\%S_{fp} = 3.3254(\%A_{fp})^{0.746} \quad (6)$$

The equations of the above investigators are for width ratio α >3.0 so significant errors are obtained when all equations are analyzed against compound channels of lower width ratio i.e $\alpha \leq$ 2.2. Following the work of previous investigators, the expression for estimating shear in floodplain has been attempted. Observing the energy gradient equation, it can be stated that SF is a function of corresponding flow area A. Then $\%S_{fp}$ of a compound channel should be a function of $\%A_{fp}$ ($\%A_{fp} = 100 \times A_{fp}/A$ where A_{fp} is the area of flood plain). Therefore, a functional relationship between $\%S_{fp}$ and $\%A_{fp}$ can be derived from data sets of five different types of compound channels with α ranging from 1.5 to 3.0. The functional correlation between $\%S_{fp}$ and $\%A_{fp}$ for the compound channel has been found out. This has been obtained by best-fit curve between $\%A_{fp}$ and $\%S_{fp}$ which gave the highest regression coefficient i.e. R^2=0.95. The data used by this model are two series of compound channel data of Knight and Demetrious (1983) , the data of experimental compound channel of NIT, Rourkela, India as well as FCF-A-03 channel, along with four series of compound channel data of Rezaei (2006) (details of the data sets are

given in Table.1). Manning's n values for all these smooth surfaces are taken as 0.01. Figure (5) shows the best fit curve and its equation is found as

$$\%S_{fp} = 3.779(\%A_{fp})^{0.691} \quad (7)$$

In terms of α, β, equation (7) can be expressed as

$$\%S_{fp} = 3.779\left[\frac{100\beta(\alpha-1)}{1+\beta(\alpha-1)}\right]^{0.691} \quad (8)$$

Following the work of Knight and Hamed (1984) the equation (8) (says present model I) can be written for non-homogeneous channel as

$$\%S_{fp} = 3.779(\%A_{fp})^{0.691}[1 + 1.02\sqrt{\beta}\log\gamma] \quad (9)$$

The deviation among the calculated values of ($\%S_{fp}$) using equations (1), (5), (6) and (8) and the subsequent observed values are shown in Figure (6). Here the accuracy of the developed model i.e. Equation (8) is verified.

The error percentage in estimating $\%S_{fp}$ is always less when compared to the result of previous models for both present experimental channel as well as channel of Rezaei (2006), Knight & Demetriou (1983) and are shown in Figure 7 (a), (b), (c) and (d) respectively.

Compound channel with Converging Flood plains

Observing equations of various researchers i.e. equation (1), (2), (6) etc. it is noticed that $\%S_{fp}$ = F (α, β, δ) for the prismatic compound channel, Where F is the functional symbol. Considerable error are observed when all the equations are verified against compound channels with converging flood plains due to variation of geometry and converging effect in such channels. So an effort has been given here to analyse the variation of $\%S_{fp}$ with respect to different geometric and hydraulic parameters of compound channels with the converging flood plain. $\%S_{fp}$ has been

evaluated from experimental data sets of three different types of converging compound channels of NIT, Rourkela, India along with data of Rezaei (2006) (details are given in Table.2). For a compound channel with converging flood plain two more parameters can be added to describe boundary shear distribution as the boundary shear distribution changes from section to section. The dependency of $\%S_{fp}$ with most influencing parameters and the best functional relationships can be expressed in the following form

$$\%S_{fp} = F\ (\alpha, \beta, \delta, \theta, X_r) \quad (10)$$

Where θ=Converging angle, X_r=Relative distance(x/L), x=distance between two consecutive sections , L=Total Non-prismatic length.

The variation of $\%S_{fp}$ with β, X_r , θ, has been plotted in different plots. The best individual relationship has been obtained as shown in Fig.8, 9 and 10.

By considering the above plots a generalized mathematical empirical relation of $\%S_{fp}$ for compound channel with converging floodplain has been modeled as

$$\%S_{fp} = 18.505 + 62.140(\beta)^{0.631} - 24.42(X_r) + 1.38(\theta) \quad (11)$$

Equation (11) represents the final expression of the model (says Model II) . More details can be found out in Naik and Khatua (2016). After finding the $\%S_{fp}$ the stage discharge relationship at different sections of a compound channel with converging floodplain can be estimated as described below.

APPLICATION OF THE MODEL

After obtaining equations to estimate $\%S_{fp}$ for the compound channel with lower width ratio for both prismatic reach and non-prismatic reach, now these can be used to predict discharge at the

prismatic and non-prismatic reach compound channels especially for lower width ratio cases. Khatua et al (2012) developed MDCM where the proportionate length of interface from the main channel and from flood plain can be evaluated by balancing the apparent shear at the vertical interface. The new expressions can be adopted instead to evaluate the momentum transfer in terms of apparent shear force occurring at the interface in terms of an appropriate length of the interface between the main channel and floodplain of a compound channel. The proportionate length of interface X_{mc} to be included in the main channel perimeter and proportionate length of interface X_{fp} to be excluded from the flood plain perimeter has been expressed as

$$X_{mc} = \mathrm{P_{mc}}\left[\frac{100}{(100-\%S_{fp})}\left(\frac{A_{mc}}{A}-1\right)\right] \quad (12)$$

$$X_{fp} = \mathrm{P_{fp}}\left[\frac{100}{\%S_{fp}}\left(\frac{A_{mc}}{A}-1\right)+1\right] \quad (13)$$

Where P_{mc} and P_{fp} are the wetted perimeters of the main channel and floodplains respectively. Further details of the derivation of equation 12 and equation 13 are found in Khatua et al (2012). After evaluating X_{mc} and X_{fp} the discharge for main channel and floodplain are evaluated using Manning's equation and added together to give over all discharge of both prismatic and non-prismatic sections of a compound channel as

$$Q = \frac{\sqrt{S}}{n_{mc}} A_{mc}^{\frac{5}{3}} (P_{mc}+X_{mc})^{-2/3} + \frac{\sqrt{S}}{n_{fp}} A_{fp}^{5/3} \left((P_{fp}+X_{fp}\right)^{-2/3} \quad (14)$$

Where S_0 is the bed slope of both main channel and floodplain and X_{mc} and X_{fp} are depending on geometrical parameters and $\%S_{fp}$. Therefore $\%S_{fp}$ can be evaluated from equation (8) and (11) respectively for prismatic compound channels and non-prismatic compound channels of lower width ratio respectively. Now, equations (8), (12), (13), (14) are used to estimate the discharge of prismatic compound channel and now let denoted as EMDCM I. Similarly equations (11), (12), (13), (14) are used to estimate the discharge of compound channel with converging flood plain

and denoted as EMDCM II. The result from EMDCM I and EMDCM II with other traditional methods like VDM, HDM, DDM are compared well when applied to the experimental channel and other data sets.

Using the equation (14), along with standard traditional methods are applied to estimate discharge in the Present experimental converging compound channel of Rourkela and Rezaei (2006) Channel both for Prismatic and non-prismatic case. Methods used are horizontal division method (HDM), vertical division method (VDM), diagonal division method (DDM). The percentage of error in estimating the discharge is computed as

$$\text{Mean } Absolute\ Error(\%) = \frac{100\%}{N} \Sigma \left| \frac{Q_{cal} - Q_{act}}{Q_{act}} \right| \quad (15)$$

Where Q_{cal} is the estimated discharge, Q_{act} is actual discharge; N is the total number of data.

After estimating discharge by different approaches with the present approach, the results are compared in Figure 11. In Figure 11, the proposed modified approach provides the best discharge result whereas HDM method is providing the worst among all methods.

Figure (12) shows the results among various methods applied to the Present experimental Channel of NIT Rourkela and Rezaei (2006) Non-prismatic channel cases. In Figure 12, the proposed modified approach provides the best discharge result whereas SCM method is providing the worst among all methods.

PRACTICAL APPLICATION OF THE METHOD

Modified Equation I (prismatic section)

After applying the modified equation I and II to the new experimental lower width channel of NIT, Rourkela and the existing narrow channel data of Rezaei (2006), it was decided to test the

approaches for its suitability in a natural river data. Therefore, the published river data of river Main (Myers and Lynness 1990) is selected in this work. The river is straight, uniform in cross section. The width ratio is less as compared to other natural rivers and it varies from 1.2 to 2.5 against the corresponding relative depth value between 0.006 and 0.47. The observed discharge ranges between 18.34 and 57.7 m^3/s. The lateral cross section of River Main has been shown in Figures (13).

The previous four standard methods have been applied to estimate discharge and the computed discharge values are then compared with actual discharge. Figure 14 shows the results of the different approaches it is seen that the present approach (EMDCM I) provide good results. Figure 14 clearly establishes the fact that EMDCM I can also be used to estimate discharge even in natural rivers having narrow flood plains with width ratio in the range of 1.5–2.2

Modified Equation II (Nonprismatic section)

For verification of the model in non-prismatic section, the River Main (Martin & Myers 1991) is chosen here. The experimental reach consists of a 1 km section of the River Main in Northern Ireland which has been reconstructed to form a compound section consisting of a central main channel and two side flood plains. A plan view of the reach was shown in Fig. 15 , which illustrates that the river was almost straight in this section. Cross-sectional dimensions of sections 14 and 6, at the limits of the reach, were shown in Fig. 16. The topographical data of these and the intermediate sections are shown in Fig. 15, were supplied by the Department of Agriculture for Northern Ireland, Drainage Division. The bed material in the main channel was coarse gravel with a D_{50} size varying from 100 mm to 200 mm, while the banks of the main

channel consist of large boulders up to 1 m in diameter. The flood plains were sown in grass. The average longitudinal bed slope of the reach was 0.003.The definitions of 'main channel' and 'flood plain' are shown in Fig.16 , showing that a vertical division had been adopted.

Geometrical properties and surface conditions of these rivers are given in Table 3. Table 4 shows the results of actual discharge and the predicted discharge using the present approach (EMDCM II) provide good results. Table 4 clearly establishes the fact that EMDCM II can also be used to estimate discharge even in natural rivers having converging flood plains.

CONCLUSIONS

1. From the experimental results on compound channels with converging flood plains, the boundary shear at the wetted perimeter for different sections are measured and the distribution of shear force carried by flood plains and in main channel perimeters were analysed. It is observed that there is a peak value of shear at the mid of the main channel and the value decreases towards the flood plains. There is a sudden drop of boundary shear value noticed at the interface. This happens to all the experimental sections covering from prismatic to non-prismatic part. But at the last section of Rezaei (2006) channel, the peak value is not at the mid of the main channel but at the interfaces in particularly at the turbulent region.

2. The shear stress percentage carried by flood plains ($\%S_{fp}$) is found to decrease from section to section of all the compound channels with converging flood plains. For the channels of the same converging angle, the shear force percentage carried by flood plains is found to increase with the increase of overbank flow depths.

3. The percentage of shear stress carried by flood plain of a lower width compound channel for prismatic part (α = 1.8) are found to be a non-linear function of the percentage of area occupied by the flood plains ($\%A_{fp}$) and the former has been expressed mathematically as a power function of the latter. The present mathematical model derived for $\%S_{fp}$ provides the least error when compared with previous models applied to lower width compound channels with width ratio ($1.5 < \alpha < 3$).

4. For a compound channel with converging flood plains mathematical expression for $\%S_{fp}$ has been expressed in terms of non-dimensional geometric and hydraulic parameters α, β, γ, θ, X_r which is specifically applicable to lower width converging compound channels.

5. The New expression of boundary shear stress distribution for the present converging compound channel has been utilized to predict the stage-discharge relationship of the compound channel for both prismatic and converging flood plains. The proposed approaches have been applied to predict discharge values for present lower width compound channel of NIT, Rourkela and Rezaei (2006) data for Prismatic and non-prismatic case. The approach is very suitable for a channel of lower width ratio and believes to predict discharge with more accuracy. Both the approaches is also found satisfactory in predicting discharge accurately in a real river case having lower width flood plains.

6. The limitation of the present work is that the new models can be utilized for prediction of the conveyance of a converging compound channel with lower width of flood plain and for homogeneous roughness in the subsections. These models can further be improved for wider flood plains and for differential roughness by utilizing more data sets for such cases.

ACKNOWLEDGMENTS

We acknowledge thankfully the support from the Institute and the UGC UKIERI Research project (ref no UGC-2013 14/017) for carrying out the experimental research work in the Hydraulics laboratory at National Institute of Technology, Rourkela.

Notation

The following symbols are used in this paper:

A = total area of the compound channel

A_{fp} = corresponding area by floodplain

B = Total width of compound channel

b = Total width of the main channel

h = Total height of the main channel

H = bank full depth

L = converging length

MAE = Mean absolute error

MAPE = Mean absolute percentage error

MSE = Mean squared error

RMSE = Root Mean squared error

S_0 = bed slope

α = width ratio (B/b)

δ = aspect ratio (b/h)

β = relative depth ((H-h)/H))

Xr = relative distance(x/L)

x = distance between two consecutive sections

θ = converging angle

S_{fp} = boundary shear carried by the floodplains

SF = total shear force of the compound channel

REFERENCES

Bousmar, D. and Zech, Y. (1999). "Momentum transfer for practical flow computation in the compound channel." J. Hydraul. Eng., 125 (7), 696-706.

Bousmar, D., Wilkin, N., Jacquemart, J.H. and Zech, Y. (2004). "Overbank flow in symmetrically narrowing floodplains." J. Hydraul. Eng., ASCE, 130(4), 305-312.

Khatua, K.K. and Patra, K.C. (2007). "Boundary shear stress distribution in compound open channel flow". J. Hydraul. Eng., ISH, 13 (3), 39–54.

Khatua, K.K.., Patra, K.C. and Mohanty, P.K.. (2012). "Stage-Discharge prediction for straight and smooth compound channels with wide floodplains. "J. Hydraul. Eng., ASCE, 138(1), 93–99.

Knight, D.W. and Demetriou, J.D. (1983). "Flood plain and main channel flow interaction." J. Hydraul. Eng., ASCE, 109(8), 1073–1092.

Knight, D.W. and Hamed, M.E. (1984). "Boundary shear in symmetrical compound channels. "J Hydraul. Eng., ASCE, 110(10), 1412-1430.

Martin, L.A., MYERS, W. Rc. (1991). "Measurement of overbank flow in a compound river channel."Proc. Instn Cio. Engrs, Part 2, 91, 645-657.

Myers, W.R.C. and Lynness, J.F. (1990). "Flow resistance in rivers with floodplains." Final report on research grants GR/D/45437, University of Ulster.

Mohanty, K. P., Khatua, K. K.and Dash, S. S. (2014). "Flow prediction in two stage wide compound channels." Journal of Hydraulic Engineering, ISH, 20 (2), 151-160.

Naik, B. & Khatua, K. K. (2016). "Boundary shear stress distribution for a converging compound channel", ISH Journal of Hydraulic Engineering, Volume 22, Issue 2.

Patel, V.C. (1965). "Calibration of the Preston tube and limitations on its use in pressure gradients.*"* J. Fluid Mech., 23(1),185–208. Cam- bridge University Press.

Proust, S., Rivière, N., Bousmar, D., Paquier, A., Zech, Y. & Morel, R. (2006). "Flow in the compound channel with abrupt floodplain contraction." J. Hydr. Eng., ASCE, 132(9), 958-970.

Rezaei, B. (2006). "Overbank flow in compound channels with prismatic and non-prismatic floodplains." PhD Thesis, Univ. of Birmingham, U.K..

Sellin, R. H. J. (1964). "A laboratory investigation of the interaction between the flow in the channel of a river and that over its flood plain." La Houilte Blanche, 7,793–801.

Figure Captions

Figure 1. (a) Plan view of experimental setup (Naik and Khatua 2016); (b) longitudinal and cross-sectional dimension of the non-prismatic compound channels; (c) grid showing the arrangement of velocity measurement points at the test section (Naik and Khatua 2016)

Figure 2. (a) Stage-discharge relationship for the Present experimental Channel (Prismatic sections); (b) stage-discharge relationship for compound channels with converging flood plains (Non-Prismatic sections of angle 12.38^0,9^0, 5^0); (c) longitudinal velocity contour for lower aspect ratio experimental channel (NITR) of relative depth 0.15(for converging angle 12.38°)

Figure 3. (a) Boundary shear distribution for lower aspect ratio experimental channel (NITR) of relative depth 0.15 (for converging angle 12.38°); (b) boundary shear distribution for higher

aspect ratio experimental channel Rezaei (2006) of relative depth 0.5 (for converging angle 11.31º) [(a and b) Naik and Khatua 2016]

Figure 4. Interface planes dividing a compound section into sub areas (Naik and Khatua 2016)

Figure 5. Variation of % of floodplain shear with % of area of floodplain

Figure 6. Scatter plot for observed and modeled value of $\%S_{fp}$

Figure 7. (a) Comparison for $\%S_{fp}$ for various models in the present experimental channel; (b) **c**omparison for $\%S_{fp}$ for various models in lower width (α=1.5) Rezaei (2006) Channel; (c) comparison for $\%S_{fp}$ for various models in lower width (α=2) Rezaei (2006) Channel; (d) comparison for $\%S_{fp}$ for various models in lower width (α=2.5) Rezaei (2006) Channel

Figure 8. Variation of $\%S_{fp}$ of floodplain shear with relative depth at typical sections (Naik and Khatua 2016)

Figure 9. Variation of $\%S_{fp}$ of floodplain shear with relative distance for different relative depths (Naik and Khatua 2016)

Figure 10. Variation of $\%S_{fp}$ of floodplain shear with converging angles for different relative depths (Naik and Khatua 2016)

Figure 11. Absolute Error of Discharge for Present experimental and Rezaei (2006) channel data (Prismatic case)

Figure 12. Absolute Error of Discharge for Present experimental and Rezaei (2006) channel data (Non-Prismatic case)

Figure 13. Lateral cross section of River Main (From CES v2.0 help manual 2007)

Figure 14. Absolute Error of Discharge of River Main

Figure 15. Plan view of experimental reach of River Main

Figure 16. Cross-sectional geometries of River Main at (a) upstream end of experimental reach (section 14); (b) downstream end of experimental reach (section 6)

Table 1 Details of geometrical parameters of the experimental and other Prismatic channels

Experimental/ other test channels	Series No.	Longitudinal slope(S)	Main channel width (b)in (m)	Main channel depth (h)in (m)	Main channel side slope	Width ratio (α= B/b)	Relative depth(β= H-h/H)	Observed discharge for lower width ratio compound channel α<3 (Q)in m^3/s
Present Channel	1	0.0011	0.5	0.1	0	1.8	0.15-0.3	0.037-0.051
Knight and Demetriou (1983)	1	0.00096	0.304	0.076	0	2	0.11-0.41	0.005-0.017
	2	0.00096	0.304	0.076	0	3	0.21-0.49	0.006-0.023
FCF Series-A-03	1	0.001027	1.5	0.15	1	2.2	0.05-0.5	0.225-0.834
Rezaei (2006)	1	0.00203	0.398	0.05	0	1.5	0.05-0.54	0.010-0.045
	2	0.00203	0.398	0.05	0	2	0.05-0.52	0.010-0.050
	3	0.00203	0.398	0.05	0	2.5	0.06-0.47	0.012-0.050
	4	0.00203	0.398	0.05	0	3	0.07-0.47	0.012-0.050

Table 2 Hydraulic parameters for the compound channels with converging flood plain data

Verified test channel	Types of channel	Angle of convergent (Θ)	Longitudinal slope (S)	Cross-sectional geometry	Total channel width (B in m)	Main channel width (b in m)	Main channel depth (h in m)	Width ratio (sec-1) B/b (α)	Converging length (X_r in m)	Aspect Ratio b/h (δ)
Rezaei (2006)	Converging (CV2)	11.31°	0.002	Rectangular	1.2	0.398	0.05	3	2	7.96
Rezaei (2006)	Converging (CV6)	3.81°	0.002	Rectangular	1.2	0.398	0.05	3	6	7.96
Rezaei (2006)	Converging (CV6)	1.91°	0.002	Rectangular	1.2	0.398	0.05	3	6	7.96
Present study	Converging	5°	0.0011	Rectangular	0.9	0.5	0.1	1.8	2.28	5
Present study	Converging	9°	0.0011	Rectangular	0.9	0.5	0.1	1.8	1.26	5
Present study	Converging	12.38°	0.0011	Rectangular	0.9	0.5	0.1	1.8	0.84	5

Table 3 Details of geometrical parameters of the experimental reach of River Main

Sl. No	Item Description	Converging Compound Channel
1	Geometry of main channel	Trapezoidal
2	Geometry of flood plain	Converging
3	Top width of compound channel (B_1)	before convergence 30.4m
4	Top width of compound channel (B_2)	after convergence 27.3m
5	Converging length of the channels	800m
6	Slope of the channel	0.003
7	Angle of convergence of flood plain (^{0})	0.138
8	Position of experimental section 1	start of the converging part
9	Position of experimental section 2	800 m away from sec-1
10	Roughness of main channel	0.035 (v.T. Chow 1959)
11	Roughness of main channel banks	0.050 (v.T. Chow 1959)
12	Roughness of flood plains	0.041 (v.T. Chow 1959)

Table 4 Details of of the experimental runs of River Main

Sections	H=total water depth	β=relative depth	calculated discharge	observed discharge	% error
14.00	1.01	0.01	16.92	18.45	8.29
14.00	1.02	0.02	17.08	19.87	14.03
14.00	1.10	0.09	18.29	19.40	5.73
14.00	1.16	0.13	19.37	21.16	8.48
14.00	1.11	0.10	18.42	21.82	15.58
14.00	1.27	0.21	22.07	28.48	22.50
14.00	1.33	0.25	23.92	31.65	24.43
14.00	1.44	0.30	27.64	37.41	26.14
6.00	0.94	0.05	15.10	16.55	8.77
6.00	0.97	0.07	15.49	15.54	0.31
6.00	1.05	0.14	16.67	18.02	7.49
6.00	1.09	0.18	17.52	19.43	9.79
6.00	1.06	0.15	16.88	19.81	14.77
6.00	1.09	0.18	17.53	21.51	18.53
6.00	1.15	0.22	18.75	20.84	10.05
6.00	1.30	0.31	22.62	29.14	22.38

Figures

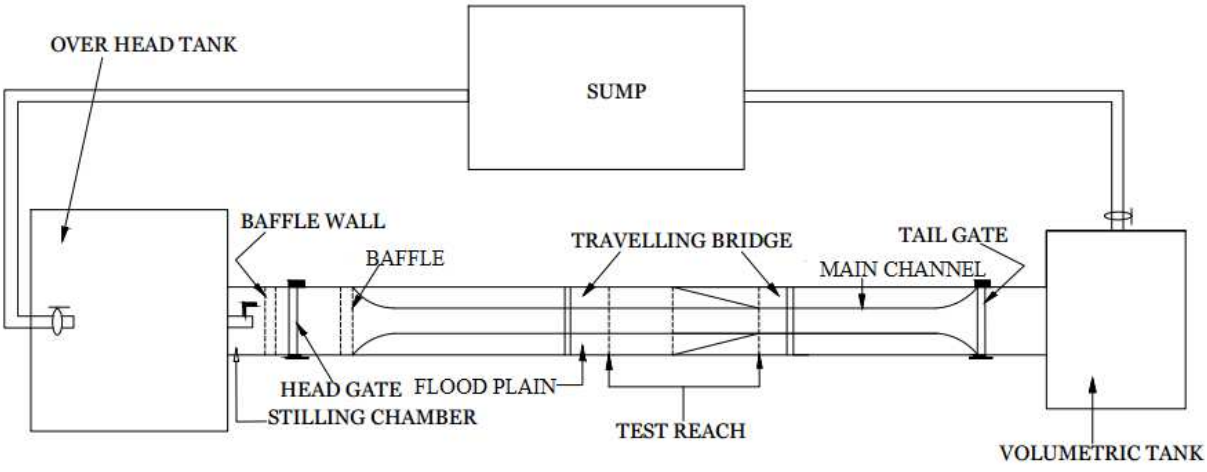

Figure 1 (a) Plan view of Experimental setup (Naik & Khatua 2016)

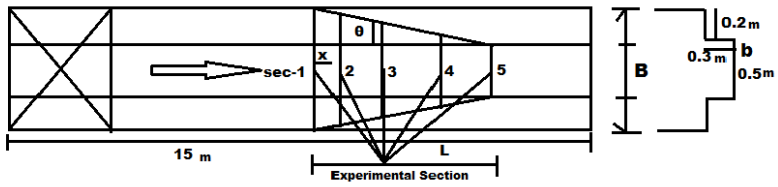

Figure1 (b) Longitudinal & Cross sectional dimension of the non-prismatic compound channels

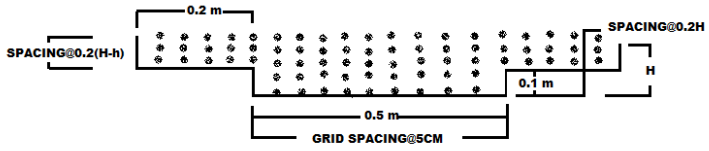

Figure 1(c) Grid showing the velocity measurement at the test section (Naik & Khatua 2016)

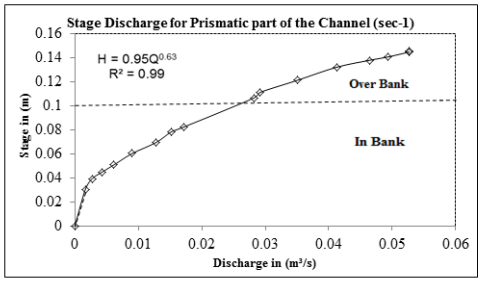

Figure 2(a) Stage discharge relationship for the Present experimental Channel (Prismatic sections)

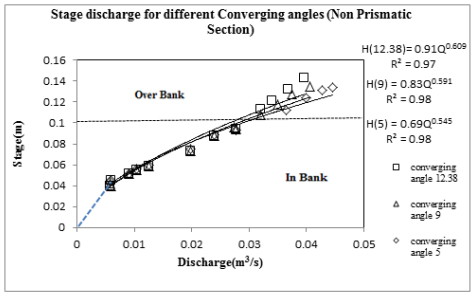

Figure 2(b) Stage discharge relationship for compound channels with converging flood plains (Non Prismatic sections of angle 12.38⁰,9⁰, 5⁰)

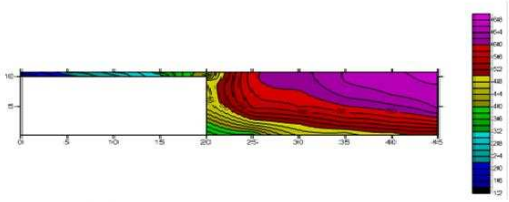

Figure 2(c) Longitudinal Velocity (cm/s) contour for lower aspect ratio experimental channel (NITR) of relative depth 0.15(for converging angle 12.38°)

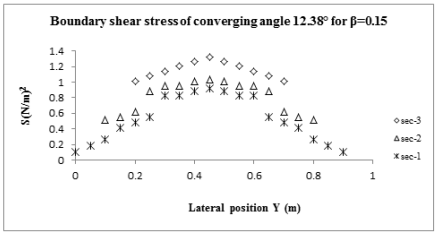

Figure 3(a) Boundary shear distribution for lower aspect ratio experimental channel (NITR) of relative depth 0.15(for converging angle 12.38°) (Naik & Khatua 2016)

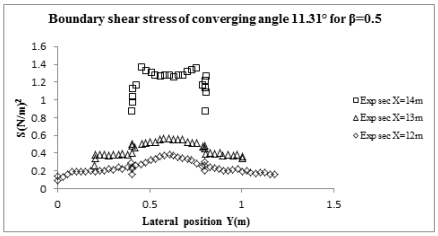

Figure 3(b). Boundary shear distribution for higher aspect ratio experimental channel Rezai(2006) of relative depth 0.5(for converging angle 11.31⁰) (Naik & Khatua 2016)

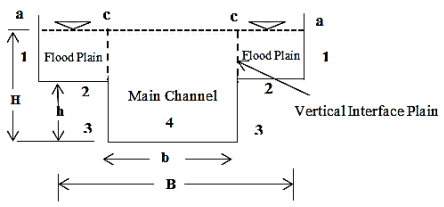

Figure 4 Interface planes dividing a compound section into sub areas (Naik & Khatua 2016)

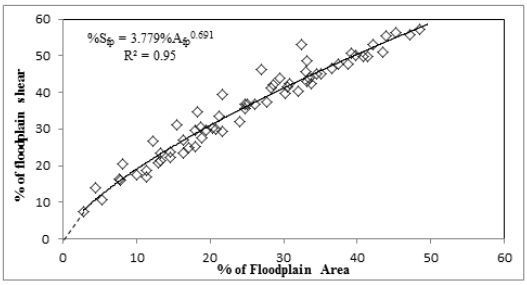

Figure 5 Variation of % of floodplain shear with % of area of floodplain

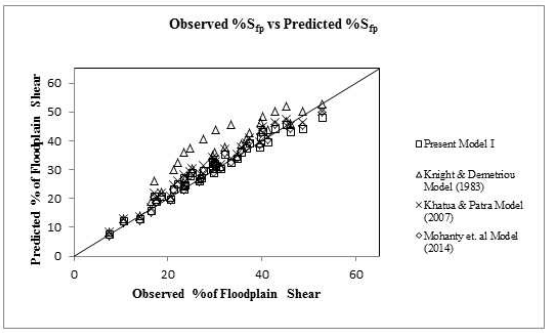

Figure 6 Scatter plot for observed and modeled value of $\%S_{fp}$

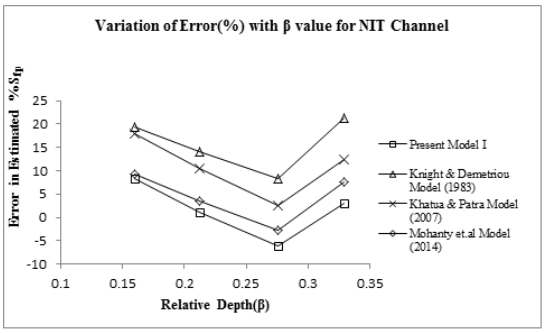

Figure 7 (a) Comparison for $\%S_{fp}$ for various models in the present experimental channel

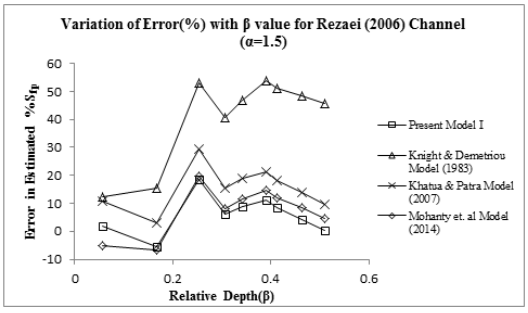

Figure 7 (b) Comparison for $\%S_{fp}$ for various models in lower width (α=1.5) Rezaei (2006) Channel

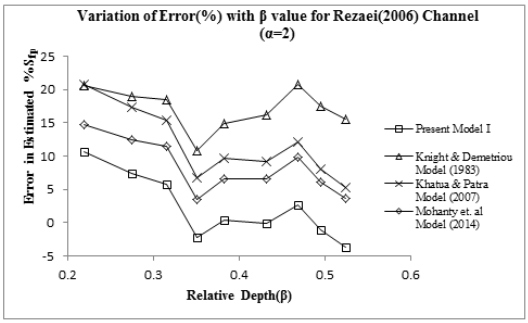

Figure 7 (c) Comparison for $\%S_{fp}$ for various models in lower width (α=2) Rezaei (2006) Channel

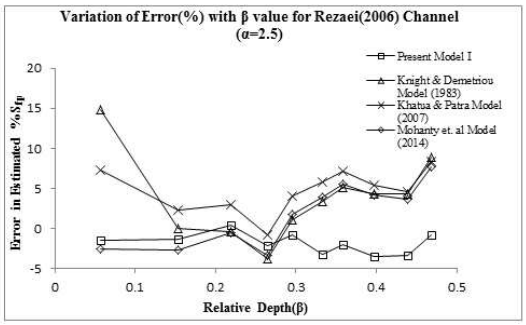

Figure 7(d) Comparison for $\%S_{fp}$ for various models in lower width (α=2.5) Rezaei (2006) Channel

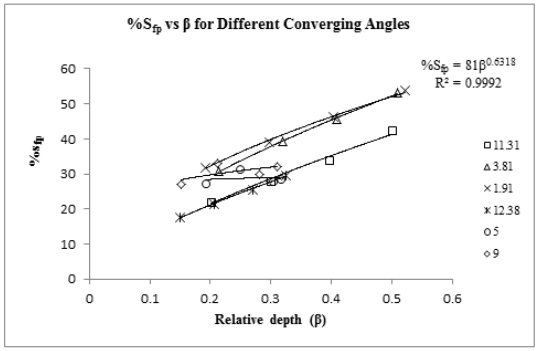

Figure 8 Variation of $\%S_{fp}$ of floodplain shear with relative depth at typical sections (Naik & Khatua 2016)

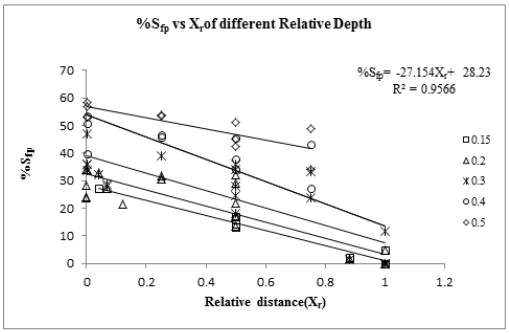

Figure 9 Variation of $\%S_{fp}$ of floodplain shear with relative distance for different relative depths (Naik & Khatua 2016)

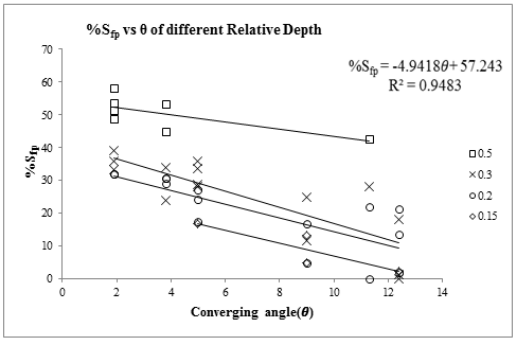

Figure 10 Variation of *%Sfp* of floodplain shear with converging angles for different relative depths Naik & Khatua (2016)

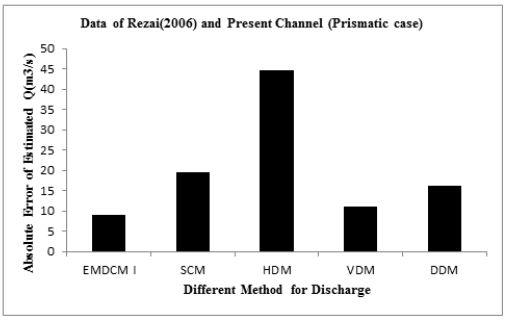

Figure 11 Absolute Error of Discharge for Present experimental and Rezaei (2006) channel data (Prismatic case)

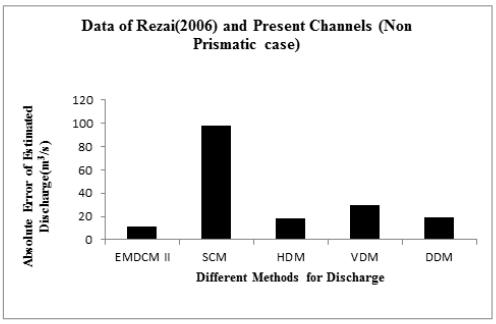

Figure 12 Absolute Error of Discharge for Present experimental and Rezaei (2006) channel data (Non Prismatic case)

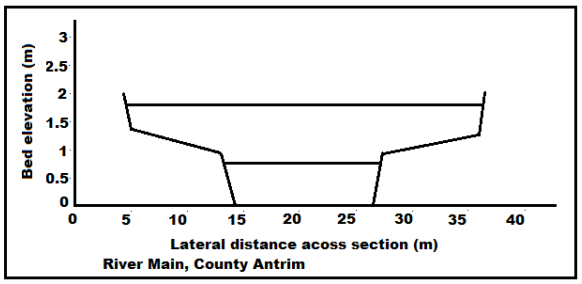

Figure 13 The lateral cross section of River Main

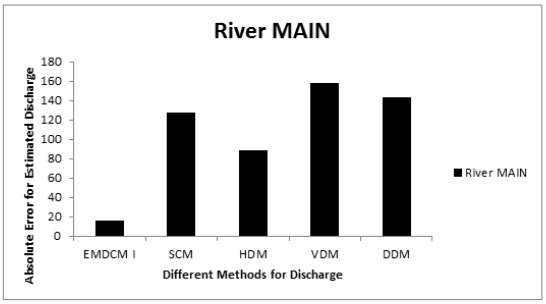

Figure 14 Absolute Error of Discharge of River Main

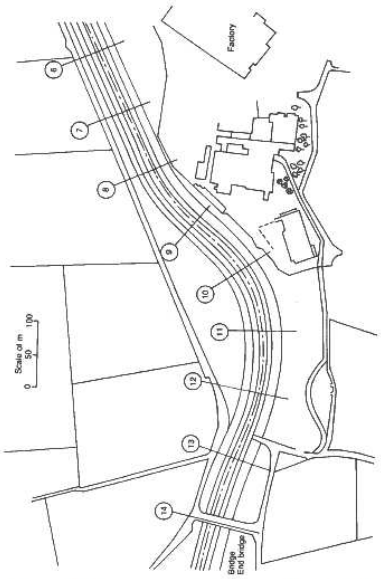

Figure 15 Plan view of experimental reach of River Main

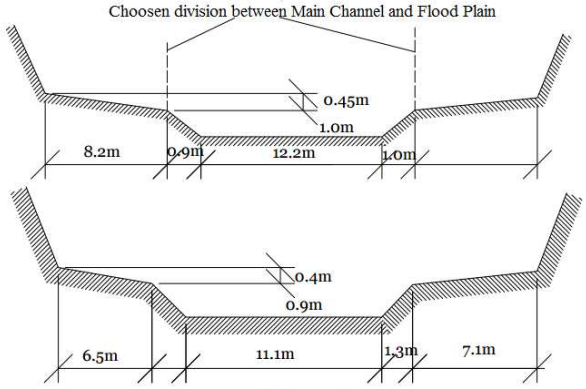

Figure 16 Cross-sectional geometries of River Main at (a) upstream end of experimental reach (section14), (b)downstream end of experimental reach (section 6)